View metadata, citation and similar papers at core.ac.uk
brought to you by CORE
provided by University of Johannesburg Institutional Repository

Some considerations for miniaturized measurement shunts in high frequency power electronic converters

A J L Joannou, D C Pentz, J D van Wyk, A S de Beer
UNIVERSITY OF JOHANNESBURG
Corner of University Road and Kingsway Road
Auckland Park, Johannesburg, South Africa
Tel.: +27 / (11) – 559.39.04.
Fax: +27 / (11) – 559.23.57.
E-Mail: aljoannou@gmail.com
URL: http://www.geep.co.za

Acknowledgements

One of the authors (A L J Joannou) would like to express gratitude to the NRF (National Research Foundation) of South Africa for financial support.

Keywords

«Component for Measurement», «Current sensor», «Measurement», «Transducer», «High frequency power converter»

Abstract

Power semi-conductors are able to achieve switching transients within a few nanoseconds and possibly even faster. These fast switching transients will need to be measured and analyzed thoroughly. In this paper four different types of shunt constructions and installations are tested on the same power electronics circuit, giving widely diverse results. Interpreting and analyzing these measurement results will assist in developing accurate current measurement devices for fast switching transient power electronic converters of the future.

1. Introduction

Wide band gap, high electron mobility transistors (HEMT), in gallium nitride (GaN) are able to switch faster than silicon (Si) based power semi-conductors [1-3]. This brings about problems with measurement of voltage and current. Although fast switching transient voltage measurement devices are available for such fast transients, current measurement methods are not as well developed in this respect. Furthermore, current measurement devices require for the measurement device to be inserted into the circuit or magnetically couple with the circuit, disturbing the setup in some or other way.

Current measurement technology below 1MHz in power converters is well established, but these devices are bandwidth limited, have a response time delay and can become complex for high frequency accuracy, and hence, the sensitivity to interference also increases. In miniature circuits, current probes and a few other methods require that a circuit wire be looped to accommodate the current measurement device. This looped conductor adds detrimental inductance to the circuit which will change the operating characteristics of the circuit at short response times. For this reason current probes and magnetic field based current measurement methods (e.g. hall-effect devices or Rogowski coils) are not discussed in this paper. The focus of this paper is resistive shunts and the effect of their construction and installation. The voltage measured across the shunt resistor is not always a direct representation of the current because of other effects, which will be discussed. As switching times reduce, these non-ideal effects become more and more pronounced until they become critical and effectively obscure the measurement. The paper discusses considerations when analyzing these voltage waveforms measured across shunts.

Consequently, the response of the voltage measured across the shunt will reveal characteristics of the shunt, as well as the dimensions, orientation and connections concerning the mounting of the shunt in the circuit. The characteristics of the shunt itself will be influenced by its external inductance in its environment as well as its internal inductance as discussed in [4]. The equivalent circuit of a current shunt is shown in Fig 1. The version of the equivalent circuit used in [5] is expanded here by considering both stored magnetic and electric energy. The parameters in Fig 1 are as follows:

$\boldsymbol{R_{shunt}(t)}$ is the total shunt resistance
$\boldsymbol{R_0}$ is the DC shunt resistance
$\boldsymbol{R_{EM}(t)}$ is the time dependent resistance due to electromagnetic wave penetration into the conductive material
$\boldsymbol{L_{shunt,ext}}$ is the external inductance of the shunt due to magnetic energy stored around the conductive material of the shunt
$\boldsymbol{L_{shunt,int}(t)}$is the internal inductance of the shunt due to magnetic energy stored in the conductive material of the shunt. This inductance is electromagnetically time dependent.
$\boldsymbol{L_{total}}$ is the sum of the installation inductance and the shunt inductance
$\boldsymbol{L_{install}}$ is the installation inductance added by inserting the shunt in the circuit
$\boldsymbol{L_{shunt}}$ is the sum of the internal and external inductances of the shunt
$\boldsymbol{C_{surr}}$ is the capacitance which models the energy stored in the electric field around the shunt
$\boldsymbol{C_{shunt}}$ is the capacitance which models the electric energy stored inside the shunt structure
$\boldsymbol{\Phi_{meas}(t)}$ is the magnetic flux which is coupled by the measurement leads
$\boldsymbol{\Phi_{total}(t)}$ is the magnetic flux which is involved with the entire shunt and installation

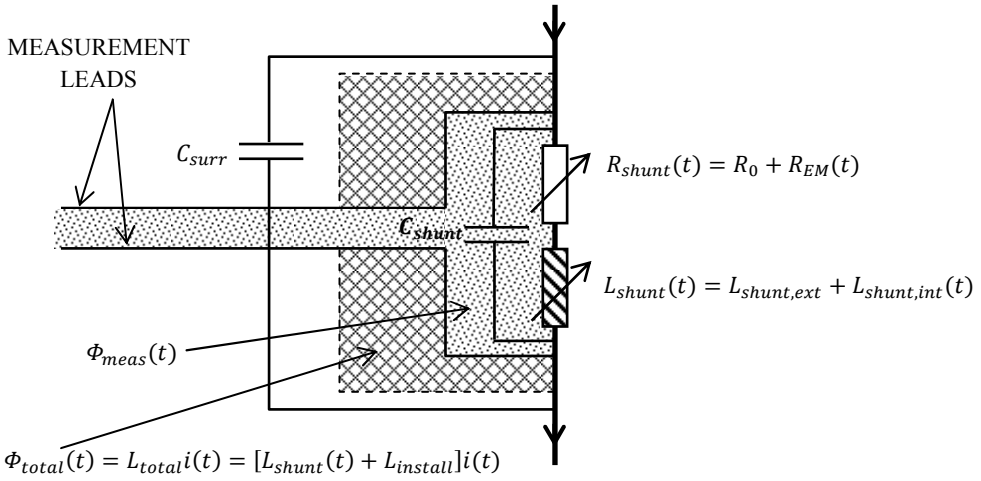

Fig 1: Expanded equivalent circuit of current shunt including external electromagnetic coupling

2. Experimental investigation

The customary frequency domain characterization of shunts will only represent the system response to steady state, single sinusoidal frequencies. The shunts are, however, intended to measure time domain, non-sinusoidal steady state converter current waveforms, in switching power electronic converters. Thus, to determine the time domain characteristics of the shunts in a circuit, the test procedure requires that a current step be applied to the shunts, and to observe their response in the time domain, as installed in the circuit.

The experimental measurements were captured using a Tektronix DPO7254 oscilloscope, which has a 2.5GHz bandwidth. The voltage across the shunts is below 5Vpeak; therefore an SMA male to SMA male coaxial cable, with a 12GHz bandwidth, was used. The source voltage, which was above 5Vpeak, was measured with a Tektronix P5050 passive voltage probe with a 500MHz bandwidth. The bandwidth specifications can be equated into a relative rise time using equation (1) as found in [6].

$$t_r = \frac{1}{\pi f_{3dB}} \tag{1}$$

The rise time information is then used to measure the fastest rise time, which can be measured with the oscilloscope and probe setup, using equation (2) and explained in more detail in [6]

$$t_{r\_min} = \sqrt{t_{r\_scope}^2 + t_{r\_probe}^2} \quad (2)$$

Using equation (2), the fastest rise time which can be measured using the oscilloscope and the SMA to SMA connector is 130ps. When measuring the source voltage with the passive voltage probe, the oscilloscope will automatically limit its bandwidth to 500MHz. Therefore the fastest rise time which can be measured is then 637ps.

A step-response test was performed and captured for each of the shunts with the same experimental setup. An EPC 9001 development board [7], using eGaN FETs, was used as a waveform generator, and is shown in Fig 2.

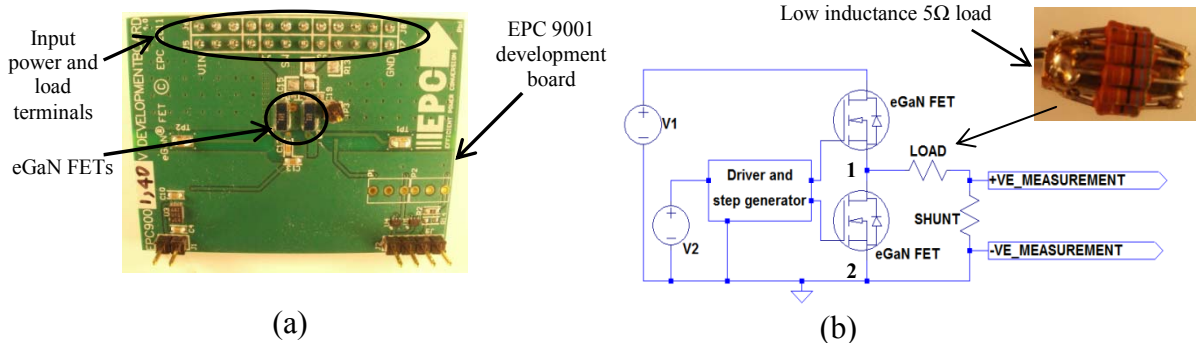

Fig 2: EPC 9001 development board (a) and experimental test setup equivalent circuit (b)

The output voltage waveform, to the combination of installed shunt and load, measured between points 1 and 2 in the schematic of Fig 2(b), is shown in Fig 3. A voltage overshoot and ringing is measured at the output voltage of the EPC9001 development board, as indicated in Fig 3. This voltage was applied to the load and shunt. The peak current output is 2A since the applied load resistor has a resistance of 5Ω.

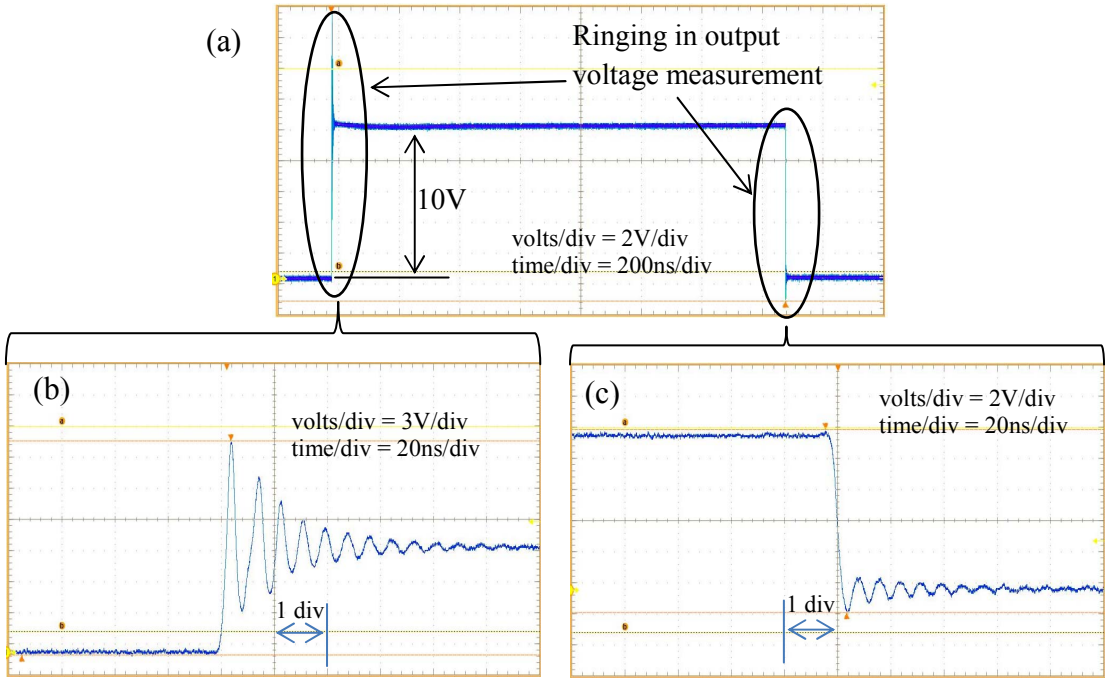

Fig 3: Output voltage of EPC9001 development board

The inductance of the load and shunt was measured in-situ, at terminals 1 and 2 of Fig 2, using an HP4284A precision LCR meter. The inductance was measured to be 60nH. The best possible rise

time with this inductance and voltage is therefore calculated for an ideal square wave of amplitude 10V:

$$V = L\frac{\Delta i}{\Delta t} \tag{3}$$

$$\Delta t = \frac{L}{V}\Delta i = \frac{60nH}{10}(2) = 12ns \tag{4}$$

Hence, the fastest current rise time of the experimental setup is 12ns.

3. Experimental results

Four different current shunt technologies were experimentally used in measurements, which demonstrate the manipulation of parasitic effects through changes in physical construction of the shunts and their circuit insertion. These results are discussed next.

3.1 Single and lateral resistor current shunt

The resistance of the single resistor shunt is 0.1Ω with a power dissipation rating of 0.125W. The step-response waveform of the voltage measured across the single resistor shunt is shown in Fig 4. Care was taken to install a miniature connector directly across the resistor, as shown in Fig 4.

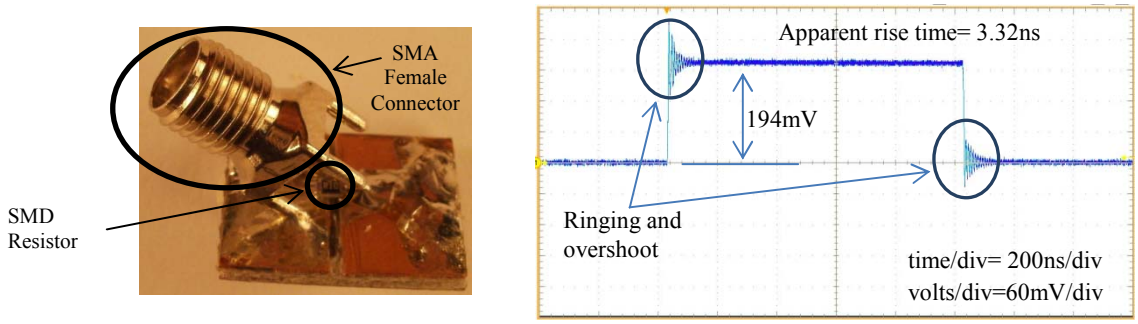

Fig 4: Single resistor shunt (a) and measurement (b)

The voltage measured across the single resistor shunt in Fig 4, shows an overshoot with ringing. This ringing can be due to the following:

i. coupling effects of the measurement leads,
ii. $\boldsymbol{\Phi_{meas}(t)}$ and $\boldsymbol{\Phi_{total}(t)}$
iii. and/or resonating inductance, $\boldsymbol{L_{shunt}}$, and capacitance, $\boldsymbol{C_{shunt}}$ and $\boldsymbol{C_{surr}}$, in the measurement setup.

These parameters are indicated in Fig 1. This overshoot can cause the measurement to appear to rise faster than the actual current through the shunt (12ns). Although this setup should contain very little stored electric energy, the stored magnetic energy around the single resistor and the measurement terminal is highly undefined. The ringing frequency is similar to the ringing frequency in Fig 3(b), meaning that the measurements have common coupling, but this is not yet fully understood. Another disadvantage of the single resistor shunt is its limited power and thermal capability.

The chosen resistor needs to be a small, thin film resistor to avoid time dependent effects such as skin effect in the shunt leading to the time dependent $\boldsymbol{L_{shunt,int}(t)}$ and $\boldsymbol{R_{EM}(t)}$. In order to measure higher currents, the actual resistor needs to be physically large or resistors are placed in parallel as in [8]. This will mean that the electromagnetic energy storage involved with the measurement will be larger, leading to a larger $\boldsymbol{C_{shunt}}$ and a larger $\boldsymbol{L_{shunt}}$. A higher power resistor also implies a thicker film, therefore skin effect will occur, hence a larger $\boldsymbol{R_{EM}(t)}$ and $\boldsymbol{L_{shunt,int}(t)}$. The result indicates that a single resistor shunt is not ideal to accurately and reliably measure non-sinusoidal fast rise time current. When the single resistor shunt is extended to higher powers by expanding into a lateral row as in [8],

the proximity effects increase $R_{EM}(t)$, $L_{shunt,int}(t)$ and $\Phi_{total}(t)$ and will come into play as well. $\Phi_{meas}(t)$ will also increase, further impairing an accurate response.

3.2 Radial lateral shunt

Another type of shunt that can be used is a radial lateral shunt as shown in Fig 5 and also presented in [9]. These shunts are electromagnetically better defined than the single resistor shunt. The current through the resistive material will be equally distributed compared to the single or lateral resistor shunts. The resistance of the radial lateral shunt was 12.5mΩ with a power rating of 2W. The same step response test was performed to the lateral shunt. The voltage measured across the lateral shunt is shown in Fig 5.

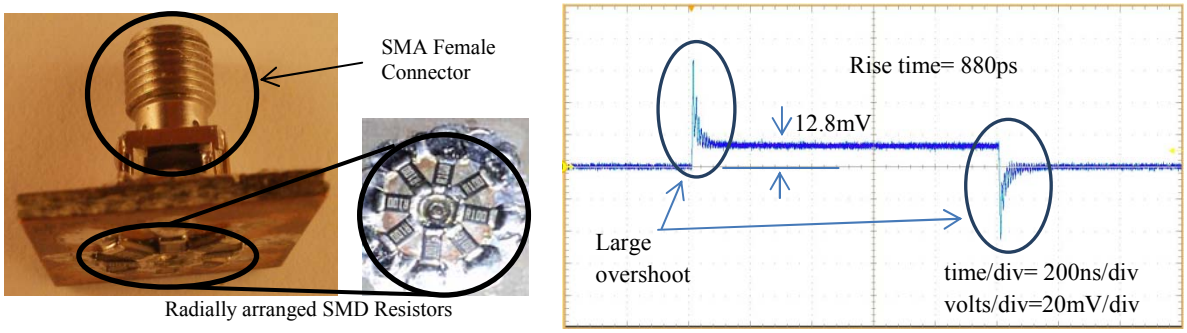

(a) (b)

Fig 5: Radial lateral shunt (a) and measurement (b)

The highly noticeable, ultra-fast rise time overshoot seen in Fig 5(b), in both the switch-on and switch-off transients already questions the ability of this shunt to measure current accurately, when the minimum theoretical rise time is 12ns. Although there is overshoot, the ringing amplitude is low, indicating good damping. This is very important because it indicates that the time dependent resistance, $R_{EM}(t)$, as shown in Fig 1, namely radial wave penetration, contributes to the overshoot. The way the current flows through the radial lateral shunt in accordance with the position from where the voltage is measured creates this overshoot. Again the ringing frequency is similar to that measured in Fig 3(b) due to common coupling.

Current flows down a co-axial via, it then spreads laterally as discussed in [9]. The current takes time to spread radially. The potential across the resistor arrangement is initially high, since the current has not yet passed through the resistors, and as the current begins to flow through the resistors, the potential decreases until the current flows uniformly throughout the structure. The inverse happens for the switch-off transient. This effect is seen as an overshoot in the measurement. The model for this effect is a time dependent resistance $R_{EM}(t)$ and time dependent inductance $L_{shunt,int}(t)$ as shown in Fig 1. The radial lateral shunt configuration will also have a high capacitance, C_{shunt}, because of its construction [9]. This is enough reason to suggest that the construction is not suitable for short rise time switching current measurement. Such a shunt can be characterized (calibrated) and used to measure sinusoidal currents, for instance in resonant converters, since the construction is such that $\Phi_{meas}(t)$ is very low.

3.3 Co-axial shunts

A common shunt used to measure large pulse currents is a co-axial shunt [4, 5]. This type of shunt is accepted as having a high bandwidth and is also electromagnetically well defined. However, passing a continuous sinusoidal current through the shunt is electromagnetically different from passing a pulse though. In the latter case, the magnetic and electric fields first have to be established in and around the structure before proper response can be obtained. If this transient time becomes comparable to the pulse rise time, then the time domain characteristics of the co-axial shunt are dependent on its dimensions. Two types of co-axial shunts were tested. A commercially available current shunt from

T&M Research Products (with part number 1M-2 which can be found in [10]) and a miniature co-axial shunt which was constructed in-house and integrated into a double sided printed circuit board.

3.3.1 T&M commercial shunt

The resistance of the T&M shunt is 10mΩ with a power rating of 20W. The step response measurement is shown in Fig 6. This shunt is physically much larger than the previous shunts discussed. Yet, unlike both the radial lateral as well as the single resistor shunt, the co-axial shunt does not show overshoot and oscillations in the measurement. The measurement is taken in the field free region and there are negligible coupling effects. $\Phi_{meas}(t)$ is effectively shielded from any stray electromagnetic fields which can interfere with the measurement. However, the shunt is much larger than the rest of the circuit, so that $L_{install}$ is inappropriately large. The slow rise time of 26.79ns is due to this effect. The datasheet for the 1M-2 co-axial model device states that this is a 2ns shunt [10], but this certainly does not take the mounting ($L_{install}$) into account. From the minimum theoretical rise time of 12ns, adding the 2ns from the datasheet [10], follows that the installation accounts for approximately 13ns, due to $L_{install}$.

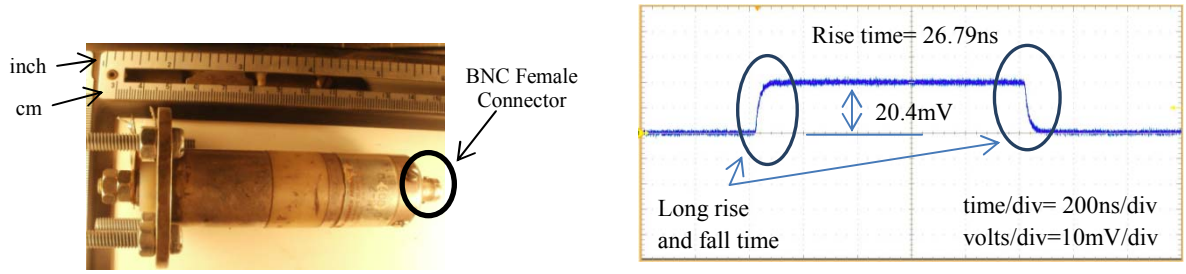

(a) (b)

Fig 6: T&M Coaxial shunt and measurement

Miniaturizing the co-axial shunt should yield better results, since this will reduce $L_{install}$ appropriately. A miniaturized shunt is discussed next.

3.3.2 Miniature co-axial shunt

A miniature co-axial shunt was constructed using SMD resistors in a hexagonal arrangement as shown in Fig 7. Fig 7 also shows a cross section of the miniature shunt indicating the current flow through the shunt, as well as where the voltage is measured across the shunt. The physically constructed shunt is shown in Fig 8.

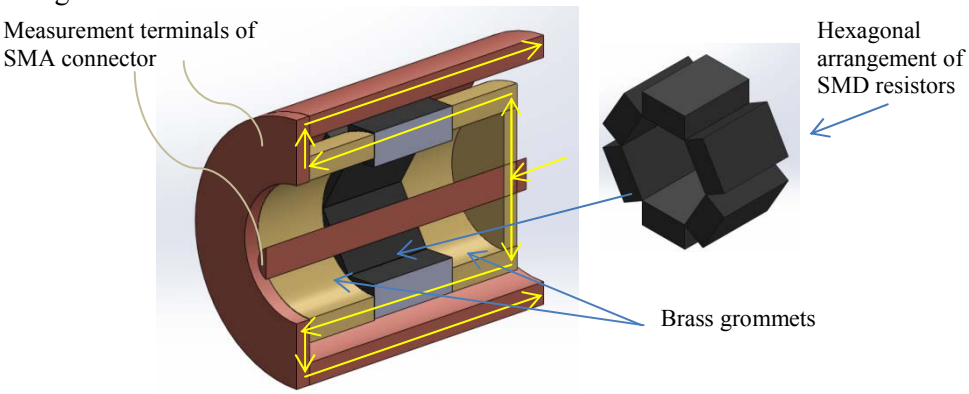

Fig 7: Miniature co-axial shunt constructed from brass grommets and SMD resistors

The miniature co-axial shunt has a power rating of 1.5W (which is much lower than the T&M co-axial shunt) and has a resistance of 16mΩ. The same step response experiment was done with this particular shunt and the result is shown in Fig 8. In the design of such a shunt, the interplay between (higher) C_{shunt}, $L_{shunt,ext}$ and the damping $R_{shunt}(t)$ may be manipulated in such a way that a critically damped response can be obtained as in [11].

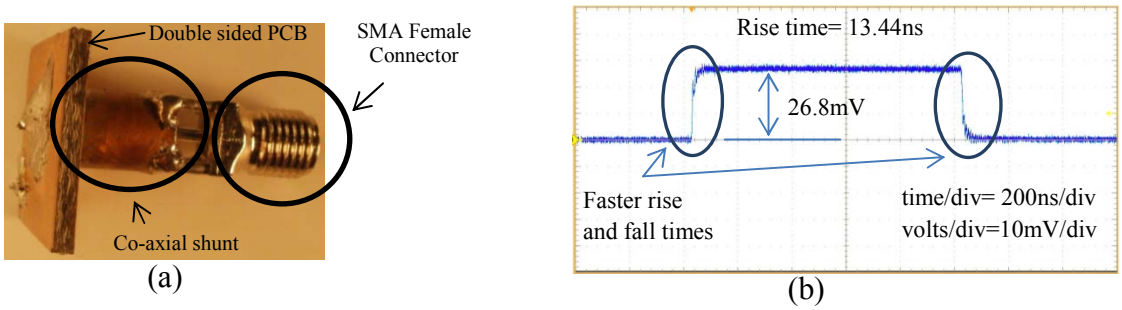

Fig 8: Miniature coaxial shunt (a) and measurement (b)

Similar to the co-axial shunt, the miniaturized version also measures no overshoot in the measurement for the same reasons as discussed for the T&M co-axial shunt. The faster rise time of L_{total}=13.44ns, compared to the T&M coaxial shunt, is evidence that $L_{install}$ is lower and accounts for a mere 1.44ns, since $L_{total} = L_{install} + L_{shunt}$. The miniature coaxial shunt has better performance than any of the other tested configurations.

4. Discussion

By using the same power electronic circuit and only changing the shunt, four rise times of 3.32ns, 880ps, 26.79ns and 13.44ns were measured. The best possible current rise time was calculated as 12ns. This indicates the enormous influence of shunt construction and installation that can falsify the measurement by either showing too short or too long rise times. The results on the in-house constructed co-axial shunt indicate that it is important to make current shunts that are electromagnetically small, for integration in future high frequency switching power electronic converters. The stored electric and magnetic energy of the shunt should be small and the wave penetration effects should be negligible compared to the rise time, so that consequently, simply making a shunt physically small does not imply it will be electromagnetically small, as indicated with the lateral and radial lateral shunt design measurements presented in this paper. The miniature co-axial current sensor discussed in this paper can integrate easily into high frequency printed circuit board designs and have been used as such.

References

[1] A Lidow.: GaN as a displacement technology for Silicon in power management, IEEE ECCE 2011, pp. 1-6

[2] A Lidow.: Is it the end of the road for Silicon in power conversion?, 6th International Conference on Integrated Power Electronics Systems, Nuremburg, Germany, March2010, pp. 461-468

[3] Nando Kaminski and Oliver Hilt.: SiC and GaN devices- competition or coexistence?, 7th International Conference on Integrated Power Electronics Systems, Nuremburg, Germany, 2012, pp. 1-11.

[4] Chucheng Xiao, Lingyin Zhao, Tadashi Asada, W G Odendaal, and J D van Wyk.: An overview of integratable current sensor technologies, IEEE IAS 2003, pp. 1251-1258.

[5] J A Ferreira, W A Cronje, and W A Relihan.: Integration of high frequency current shunts in power electronic circuits, IEEE Transactions on Power Electronics Vol. 10 no. 1, pp. 32-37

[6] H Johnson, M Graham.: High-speed digital design a handbook of black magic, Prentice Hall PTR, 1993.

[7] Efficient Power Conversion Corporation, Inc. (2013) EPC- Efficient Power Conversion. [Online]. http://epc-co.com/epc/Products/DemoBoards/EPC9001.aspx

[8] Milisav Danilovic et al.: Evaluation of the Switching Characteristics of a Gallium-Nitride Transistor, IEEE ECCE 2011, pp. 2681-2688

[9] A LJ Joannou and D C Pentz.: Miniature integrated co-axial current shunt for high frequency switching power electronics, SAUPEC 2013, South Africa, pp. 140-145

[10] T&M Research Products. T&M RESEARCH PRODUCTS. [Online]. http://www.tandmresearch.com/

[11] H Luehrmann and R Malewski.: Sprungantwort und Antwortzeit rohrformiger koaxialer Strom-Messwiderstaende beliebiger Wandstaeke," Archivfuer Elektrotechnik Vol. 75, no. 3, pp. 111-118, 1975.